Temperature Field Reconstruction of Flame from Images for Optimal Energy-Efficient Control of the Air-Fuel Mixture Making in Steam – Driven Boilers

O. B. Ospanov(✉), D. L. Alontseva, and A. L. Krasavin

Department of Instrument Engineering and Technology Process Automation,
D. Serikbayev East Kazakhstan State Technical University,
Protozanov 69, 070004 Ust-Kamenogorsk, Kazakhstan
ospanovolzhas@gmail.com, dalontseva@mail.ru, alexanderkrasavin@mail.ru

Abstract. Over recent years, substantial efforts have been made to develop technologies for the flame 3D reconstruction and characterization. Among those, the digital image based on tomographic technique has received great attention due to its clear advantages over other approaches. The technology of digital image appeared to be the most suitable for the 3D measurement of flame in practical furnace. Digital image-based tomography of flame can be achieved using either a single camera or multi-camera set-up. Although the single camera approach is simple in structure and low in cost, it can only be applied under strict conditions where the flame is steady and has a high level of rotational symmetry. For the more accurate reconstruction of unsteady and asymmetric flame, a multi-camera system has to be employed. The process of capturing the light from a combustion flame onto an imaging sensor is physically equivalent to a Radon transformation where a 2D flame cross-section undergoes transformation to produce a 1D section projection. Consequently, the reconstruction of a flame cross-section from its multiple 1D projections turns out to be the inverse Radon transformation. Among the majority of currently known multi-camera optical pyrometry methods for temperature field reconstructing, the back-projection algorithm is used for Radon inverse transformation. At the same time, the back-projection algorithm is known to have a low accuracy of restoring the original distribution. The purpose of this report is a study of the algebraic approach possibilities to numerical Radon inverse transformation. We hope that the proposed method can be useful in the process of the 3D image temperature field reconstructing.

Keywords: Two-colorpyrometry · Flame · Temperature field reconstruction · Radon transform · Inverse Radon transform · Numerical methods

Y. Shokin and Z. Shaimardanov (Eds.): CITech 2018, CCIS 998, pp. 171–180, 2019.
https://doi.org/10.1007/978-3-030-12203-4_17

1 Introduction

In recent years, a large amount of research has been focused on the development of automatic process control systems in thermal power plants (CHP). The main control task for the CHP is the following: the automatic control system must regulate the output power to meet the electricity demand in combination with the safe maintenance of the required values of the main dynamic variables such as steam heater temperature, throttle pressure, furnace pressure, and drum water level. As a rule, this goal is achieved through the use of multi-level automatic controllers based on proportional-integral-differential (PID) controllers [1–3]. This approach turns out to be highly reliable and provides satisfactory performance during normal operation, maintained in the system, where the characteristics of CHP plants remain almost constant. However, the demand for electricity increases, while the magnitude of the cyclic change in the grid load of renewable sources such as wind, solar and hydropower, is strongly influenced by the season and weather conditions. Consequently, CHP must participate in the overall energy production network and respond to these changes by adjusting the load in a wide and rapidly changing wide range. Thus, the above thermal parameters of CHP plants should be monitored so that they can work optimally at any time. At present, the problems of control in conditions of non-linearity of parameters in a wide range of operations, high inertia and time-varying behavior, as well as strong interaction among a multitude of variables, are becoming serious challenges for CHP process control systems. Consequently, conventional PI/PID controllers based on controllers are already insufficient for the required performance, even if they are well tuned at a given load level. On the other hand, with the help of modern computer and instrumental technologies and the use of a distributed control system, it is now possible to introduce advanced intelligent controllers. Intelligent control systems developed on the basis of neuro-fuzzy networks are described in papers [4–6], where both linear models and controllers are given and evaluated. Thanks to simulation studies of a coordinated control system for a boiler-turbine system and a superheater controlled by an intelligent controller, higher control values are shown in comparison with linear intelligent systems of general control.

The authors of this work are developing an intelligent controller to control the processes of formation of the fuel-air mixture in steam boilers, including a “fast” temperature control circuit based on the readings of the pyrometer. A radiation detector is used as a detector, the selected detection wavelength depends on the type of fuel burned, the operation of the device and the circuits are described in more detail in our paper [7].

It has been proved that the geometric, luminous, and fluid dynamic characteristics of the flame in combustion systems are closely related to combustion efficiency and pollutant emissions as well as furnace safety [8]. Advanced monitoring and characterization of these flames have therefore become increasingly important for engineers to better understand and optimize combustion processes. In recent years, much research effort has been directed towards the development of advanced instrumentation systems for enhanced monitoring and specification

of flames, particularly with the latest optical sensing, digital imaging, and image processing techniques [9]. However, the flame data obtained from these systems is limited to two dimensions (2-D) only, i.e., the third dimension has not been taken into account. The most recent advance in this area of research is the development of an instrumentation system for three-dimensional (3-D) visualization and quantitative characterization of red gas flames [9,10]. However, the system was elaborated to measure geometric and luminous parameters of flames from a reconstructed 3-D flame model, ignoring 3-D temperature information. Accurate measurement of temperature distribution in combustion flames is necessary to achieve fundamental understanding of combustion and polluting substances formation processes. Three-dimensional temperature measurement of combustion flames is of a major technical challenge. As a result, very limited scope of work has previously been reported on the subject. It is the nature of combustion flames which is the greatest problem in attempting to determine any information as to their internal structure in 3-D, including temperature. Moreover, as translucent, a flame cannot be inspected and analyzed using established 3-D techniques, such as tomography as used in medical imaging. Previous work in the area includes theoretical study on the determination of 3-D temperature distribution in a large furnace using multiple cameras [11]. However, the principles upon which the described system is based appear to be difficult for implementing the system.

The purpose of this study is to develop a mathematical apparatus for the reconstruction of the three-dimensional temperature field of the flame, which is being formed in an industrial boiler and controlled according to the readings of the pyrometer.

2 Principles of Two-Color Pyrometry

Pyrometry is based on the fact that all surfaces at temperatures above absolute zero emit thermal radiation. Planck's radiation law (1), modified to include surface emissivity, is the fundamental relation of thermal radiation:

$$M(\lambda, T) = \epsilon_\lambda \frac{C_1}{\lambda^s (e^{\frac{C_2}{\lambda T}} - 1)}, \tag{1}$$

where $M(\lambda, T)$ is the monochromatic exitance, namely monochromatic radiation measured in ration of energy per unit area per unit time (W/m2/s), λ is the wavelength of the radiation (mm), T is absolute temperature (K), ϵ_λ is monochromatic emissivity, and C_1 and C_2 are the first and second Planck's constants. In cases $\frac{C_2}{\lambda T} \gg 1$, Planck's law can be replaced by the Wien's radiation law (2):

$$M(\lambda, T) = \epsilon_\lambda \frac{C_1}{(\lambda^s)^5} e \frac{C_2}{\lambda T}. \tag{2}$$

It can be shown that the output of the imaging system, namely the grayscale $G(\lambda, T)$, is proportional to the exitance of the measured object and dependent on the spectral sensitivity S_λ of the imaging system (CCD sensor), i.e.,

$$G(\lambda, T) = RS_\lambda \epsilon_\lambda \frac{C_1}{(\lambda^s)^5} e \frac{C_2}{\lambda T}, \tag{3}$$

where R is called the instrument constant which is independent of wavelength and reflects the effects of various factors including radiation attenuation due to the optical system and atmosphere, observation distance, lens properties and signal conversion. The ratio between the grey levels at wavelengths λ_1 and λ_2 is given by Eq. (4):

$$\frac{G(\lambda_1, T)}{G(\lambda_2, T)} = \frac{S_{\lambda_1} \epsilon_{\lambda_1}}{S_{\lambda_2} \epsilon_{\lambda_2}} (\frac{\lambda_2}{\Lambda_1})^5 \exp{(\frac{C_2}{T}(\frac{1}{\lambda_2} - \frac{1}{\lambda_1}))} \tag{4}$$

The ratio between the spectral sensitivities $\frac{S_(\lambda_2)}{S_(\lambda_1)}$ is called instrument factor and is known from calibration using a tungsten lamp as a standard temperature source. A crucial point here is how to deal with the ratio between the spectral emissivities λ_1 and λ_2. Normally, gray body behaviour is assumed for the detected object (i.e., $\frac{\lambda_2}{\lambda_1} = 1$), when the wavelengths are very close to each other. For gaseous flames, the size of the soot particles ranges from 0.005 to 0.1 mm [5] and is much smaller than the wavelengths of observation. Flower (1983) proved that, when assuming the soot particles in the flame to be homogeneous, optically thin, isothermal along a horizontal line through the flame, and small relative to the used wavelength, the spectral emissivity is inversely proportional to the wavelength, i.e., $\lambda_1 \backsim \frac{1}{1}$. Therefore, another formulation for gaseous flames in this study is obtained by substituting $\frac{\lambda_2}{\lambda_1} = \frac{e_(\lambda_2)}{e_(\lambda_1)}$ into Eq. (5):

$$T = \frac{C_2(\frac{1}{\lambda_1} - \frac{1}{\lambda_2})}{\ln \frac{G(\lambda_1, T)}{G(\lambda_2, T)} + \ln \frac{S_{\lambda_2}}{S_{\lambda_1}} + \ln (\frac{\lambda_1}{\lambda_2})^6} \tag{5}$$

3 Principle of Measurement

Two-color pyrometry has been used extensively in many combustion applications but its application is relatively new to coal flames. Reviews and discussions on the uncertainties of the two-color method for measuring temperature and KL can be found by Ladommatos and Zhao [12] and others [13–16]. the two colors can be derived by several methods. The simplest is to obtain emission from a single line of sight (provides a point measurement) which is split and then optically altered to produce two narrow bands of light. Shaw and Essenhigh [17] used this method on a laboratory scale reactor using pulverized coal to yield point temperature measurements. Lu and Yan [9] used a single, CCD camera to measure the two-dimensional (2D) temperature in a 500 kW pulverized-coal flame. The light from the flame was split and altered into three narrow wavelength beams and captured by the CCD detector on the camera. The signals for the three beams were processed continuously to provide online temperature readings. The effects on temperature with varied air-fuel ratios, fuel low rates, and particle sizes were examined. Huang et al. [18] used a similar method to yield 2D, continuous

temperature measurements using a single CCD camera with rotating, narrow (10 nm) band-pass filters. Three hundred images were taken over a period of thirty seconds with each band-pass filter. The signals for each wavelength were averaged and then used to compute the average, 2D flame temperature. In order to calculate the temperature distribution of a flame cross section from its gray scale images using the two-color method, it is necessary to reconstruct two gray scale representations of the cross section for two different spectral bands (Fig. 1).

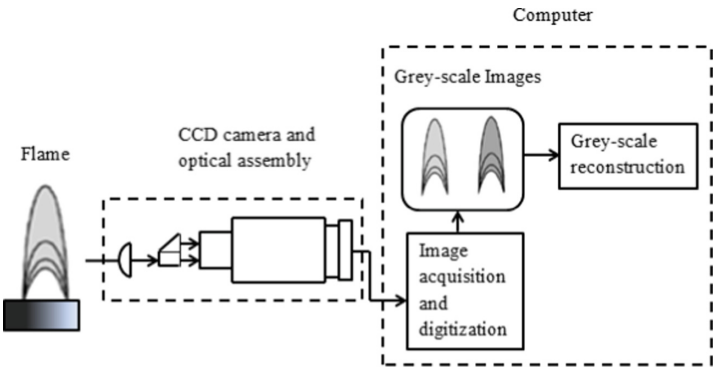

Fig. 1. Functional schematic of the two-color pyrometer

The process of projecting the light from a combustion flame onto an imaging sensor is physically equivalent to a Radon transformation, where a 2-D flame cross section undergoes transformation to produce a 1-D section projection [19]. Consequently, the reconstruction of a flame cross section from its 1-D projection is essentially the inverse Radon transformation. As a matter of fact, the implementation of the inverse Radon transformation requires infinitely many of projections from a 180 arc around the burner axis. In practice, however, the reconstruction is achieved using a sufficiently large number of projections (Fig. 2).

4 Radon Transform

Let $f(x, y)$ be a function of two real variables defined on the whole plane, and decreasing sufficiently fast at infinity (so that the corresponding improper integrals converge). Then by the Radon transform of the function $f(x, y)$ is defined as (6)

$$R(s, \alpha) = \int f(s\cos\alpha - z\sin\alpha, s\sin\alpha + z\cos\alpha)\, dz \tag{6}$$

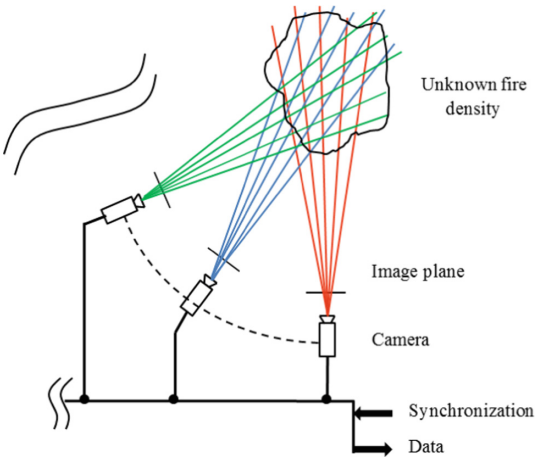

Fig. 2. Schematic illustration of the reconstruction problem

The geometric meaning of the Radon transform is the integral of the function along a straight line perpendicular to the vector$n = (\cos\alpha, \sin\alpha)$ and passing at a distance s (measured along the vector n, with the corresponding sign) from the origin (Fig. 3)

The Radon transform can be defined in different ways. The Radon transform $q^{\widehat{}}(\rho, \tau)$ of a continuous two dimensional function $q(x, y)$ is found by stacking or integrating values of g along slanted lines. The location of the line is determined from the line parameter: slope ρ and line τ offset.

$$q^{\widehat{}}(\rho, \tau) = \int q(x, \rho x + \tau)\, dx \tag{7}$$

We will use

$$S(\rho, \varphi) = \iint f(x, y)\delta(\rho - x\cos\varphi + y\sin\varphi)\, dxdy, \tag{8}$$

where $\delta(\rho)$ is a Dirac's delta-function.If the distribution function $f(x, y)$ is known, the formula (8) allows to calculate so-called "sinogram" $S(\rho, \varphi)$.

5 Numerical Inversion of Radon Transform

The inverse task means that to find $f(x, y)$ when the function $S(\rho, \varphi)$ is known. There is an exact solution of Eq. (1), which was found by Radon himself. It is called inverse Radon transform and has the form (9):

$$f(x, y) = -\frac{1}{2\pi^2} \int_0^{\pi} d\varphi \int \frac{DS}{D\rho} \frac{d\rho}{\rho - x\cos\varphi + y\sin\varphi} \tag{9}$$

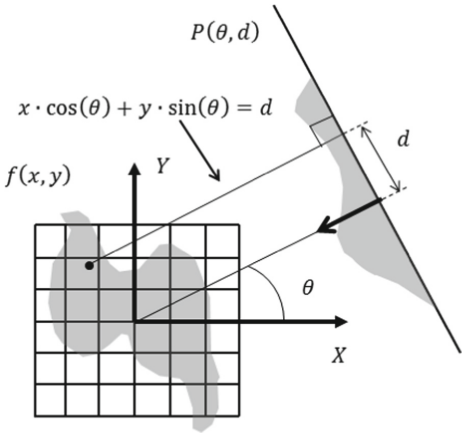

Fig. 3. Geometry of the Radon transforms

It should be noticed, that the method of Radon transform is widely used in tomography [20]. Its main advantage is that there is no need to solve the system of algebraic equations. This method gives the explicit expression for the density function $f(x, y)$ through the ray-sums of sinogram $S(\rho, \varphi)$, Of course the matter is not reduced to find the inverse operator for Eq. (12), which is incorrect. Currently, the most common method of numerical inversion of the Radon transform is the inverse projection algorithm [21,22]. In any case we can get the corresponding expression by using different mathematical transformations and hypotheses. It seems that those transformations must be examined in detail and replaced by its approximated matrix analogs. In theory of Radon transform there is an interesting ratio, which gives an integral equation to find the phantom density. Let consider double integral on a plane (10):

$$I(q, x, y) = \iint\limits_{D} \frac{f(\alpha, \beta)}{\sqrt{(x-\alpha)^2 + (x-\beta)^2 - q^2}} \, d\alpha d\beta, \tag{10}$$

where D defined as $(x-\alpha)^2 + (x-\beta)^2 > r^2$

Let's

$$\alpha = x + r\cos\theta \beta = y + r\sin\theta \tag{11}$$

Then (11) transforms to

$$\int\limits_{r}^{\infty} \frac{r\,dr}{\sqrt{r^2 - q^2}} \int\limits_{0}^{2\pi} (x + r\cos\theta, y + r\sin\theta)\, d\theta = I(q, x, y) \tag{12}$$

The internal in (12) is a mean density along circles with radius r > q, that means

$$f^{\widehat{=}}(r, x, y) = \frac{1}{2\pi} \int\limits_{0}^{2\pi} (x + r\cos\theta, y + r\sin\theta)\, d\theta \tag{13}$$

Thus, expression (13) is an integral equation to determine unknown function $f(r, x, y)$:

$$\int_r^\infty \frac{f^{\widehat{=}} r dr}{\sqrt{r^2 - q^2}} = \frac{1}{2\pi} I(q, x, y) \tag{14}$$

Last equation is a well-known Abel equation, and its solution is expressed by formula:

$$f^{\widehat{=}}(r, x, y) = \frac{1}{\pi^2} \int_r^\infty \sqrt{r^2 - q^2} \left(\frac{DI}{Dq}\right) dq \tag{15}$$

For $r \to 1$: the mean density naturally converted to the density in point (x, y), and we get:

$$f(x, y) = -\frac{1}{\pi^2} \int_r^\infty \frac{1}{q} \left(\frac{DI}{Dq}\right) dq \tag{16}$$

If we know relation between distances q and detector numbers p, then the function $I(q, x, y)$ can be written through the sinogram in form

$$I(q, x, y) = \int_0^{2\pi} S(\rho, \varphi)\, d\varphi \tag{17}$$

Hence, the phantom density (17) can be presented as (18):

$$f(x, y) = \int_0^{2\pi} d\varphi \int \frac{DS}{D\rho} \frac{d\rho}{q(\rho, \varphi, x, y)} \tag{18}$$

The value q, included into (7) is a distance from each image point (x, y) to each ray (ρ, φ) passing camera. The elements of four dimensional array q can be calculated by formula (7). For its practical usage one can introduce three dimensional array of inversed distances $Q(\alpha, x, y)$. In formula (6), which made the Radon transform, exist a numerical operation of differentiation of sinogram $S(\rho, \varphi)$ by detectors ρ. If ρ considered as number of lines, and φ - as number of columns, then numerical differentiation is more comfortable do by multiplication of $S(\rho, \varphi)$ from left on the corresponding matrix M, i.e. $S_1(\rho, \varphi) = DS(\rho, \varphi) = MS(\rho, \varphi)$. In the internal points of differentiated vector-column the derivative is approximated by central differences, but in extreme points - one-side differences. The matrices of differentiation operator M can be built with any sizes. They are distinguished from Toeplitz matrices, having the same values on diagonals, by the first and last lines.

The main results of this research are following:

(1) The mathematical approach of the two-color pyrometry task with usage matrix algorithm for 3D temperature field reconstruction was formulated.

(2) In contrast to the known approaches, the matrix algorithm gives precise reconstruction of the radiation intensity distribution. However, it is sensitive to the inaccuracy of image parameters. This drawback is also inherent for other image based pyrometry methods.
(3) We have currently tested the possibility of using the direct method of solving the inverse Radon equation in combination with the recently developed regularization methods.

6 Conclusion

A mathematical apparatus has been developed to recreate the three-dimensional temperature field of the flame, which is being formed in an industrial boiler unit and controlled according to the readings of the pyrometer. The two-color pyrometry problem is solved using the matrix algorithm for the recovery of a three-dimensional temperature field using direct and inverse Radon transforms. In practice, the developed methods are used to create an intelligent system for managing the processes of forming a fuel-air mixture in steam boilers, including a "fast" temperature control circuit with an intelligent controller that works with pyrometer readings.

The results of the research are of significance for a wide range of researchers developing temperature control circuits using pyrometers.

References

1. Xiao, W., Jiong, S., Yiguo, L., Kwang, Y.L.: Steam power plant configuration, design, and control. In: WIREs Energy Environ, p. 27. Wiley, Hoboken (2015)
2. Mallik, A.: State feedback based control of air-fuel-ratio using two wide-band oxygen sensors. In: Proceedings of 10th Asian Control Conference (ASCC 2015), Kota Kinabalu, Malaysia, pp. 1–6 (2015)
3. Najimi, E., Ramezani, M.H.: Robust control of speed and temperature in a power plant gas turbine. ISA Trans. **51**, 304–308 (2012)
4. Li, X., Guan, P., Chan, C.W.: Nonlinear multivariable power plant coordinate control by constrained predictive scheme. IEEE Trans. Contr. Sys. Technol. **18**, 1116–1125 (2010)
5. Liu, X.J., Chan, C.W.: Neuro-fuzzy generalized predictive control of boiler steam temperature. IEEE Trans. Energy Conver. **21**, 900–908 (2006)
6. Liu, X., Liu, J.: Constrained power plant coordinated predictive control using neurofuzzy model. Acta Autom. Sinica **32**, 785–790 (2006)
7. Ospanov, O.B., Alontseva, D.L. Krasavin, A.L.: Development of an intelligent system for optimal energy-efficient control of the air-fuel mixture making in steam - driven boilers. In: The Joint Issue of Journals "Herald of D. Serikbayev EKSTU" and "Computational Technologies", vol. 1, no. 2, pp. 56–70 (2018)
8. Toftegaard, M.J., Brix, J., Jensen, P.A., Glarborg, P., Jensen, A.D.: Oxy-fuel combustion of solid fuels. Prog. Energy Combust. Sci. **36**(5), 581–625 (2010)
9. Lu, G., Yan, Y.: Temperature profiling of pulverized coal flame using multicolor pyrometric and digital imaging techniques. IEEE Trans. Instrum. Meas. **55**(4), 1303–1308 (2006)

10. Brisley, P.B., Lu, G., Yan, Y., Cornwell, S.: Three dimensional temperature measurement of combustion flames using a single monochromatic CCD camera. IEEE Trans. Instrum. Meas. **54**(4), 1417–1421 (2005)
11. Zhou, H.C., Han, S.D., Lou, C., Liu, H.: A new model of radiative image formation used in visualization of 3-D temperature distributions in large-scale furnaces. Numer. Heat Transfer B Fundam. **42**(3), 243–258 (2002)
12. Ladommatos, N., Zhao, H.: A guide to measurement of flame temperature and soot concentration in diesel engines using the two-colour method, part 1. In: SAE Paper, vol. 941956 (1994)
13. Ladommatos, N., Zhao, H.: A guide to measurement of flame temperature and soot concentration in diesel engines using the two-colour method, part 2. In: SAE Paper, vol. 941956 (1994)
14. di Stasio, S., Massoli, P.: Influence of the soot property uncertainties in temperature and volume-fraction measurements by two-colour pyrometry. Meas. Sci. Technol. **5**, 1453–1465 (1994)
15. Zhao, H., Ladommatos, N.: Optical diagnostics for soot and temperature measurement in diesel engines. Prog. Energy Combust. Sci. **24**(3), 221–225 (1998)
16. Tree, D.R., Svensson, K.I.: Soot processes in compression ignition engines. Prog. Energy Combust. Sci. **87**, 272–309 (2007)
17. Shaw, D.W., Essenhigh, R.H.: Temperature fluctuations in pulverized coal (P.C.) flames. Combust. Flame **86**, 333–346 (1991)
18. Huang, Y., Yan, Y., Riley, G.: Vision-based measurement of temperature distribution in a 500-kW model furnace using the two-colour method. Measurement **28**, 175–183 (2000)
19. Lou, C., Zhou, H.C., Yu, P.F., Jiang, Z.W.: Measurements of the flame emissivity and radiative properties of particulate medium in pulverized-coal-fired boiler furnaces by image processing of visible radiation. Proc. Combust. Inst. **31**(2), 2771–2778 (2007)
20. Faridani, A.: Tomography and sampling theory, the radon transform and applications to inverse problems. In: AMS Proceedings of Symposia in Applied Mathematics. American Mathematical Society, Providence (2006)
21. Jia, R.X., Xiong, Q.Y., Wang, K., Wang, L.J., Xu, G.Y., Liang, S.: The study of three-dimensional temperature field distribution reconstruction using ultrasonic thermometry. AIP Adv. **6**(7), 075007 (2016)
22. Li, Y., Liu, S., Inaki, S.H.: Dynamic reconstruction algorithm of three-dimensional temperature field measurement by acoustic tomography. Sensors **17**(9), 2084 (2017)